

Clumps of randomly charged polymers: Molecular dynamics simulation of condensation, crystallization, and swelling

Motohiko Tanaka¹ and Toyochi Tanaka²

¹*National Institute for Fusion Science, Toki 509-5292, Japan*

²*Department of Physics, Massachusetts Institute of Technology, Cambridge, Massachusetts 02139*

(Received 24 February 2000; revised manuscript received 17 April 2000)

The behavior of randomly charged polyampholytes against a wide range of the Coulomb coupling parameter Γ (the ratio of the Coulomb energy to thermal energy) is studied with the use of molecular dynamics simulations. Neutral polyampholyte collapses for $\Gamma > 1$, where large volume changes are due to multichain effects. Charged chains reptate significantly in a globule. Polyampholyte with widely extensible bonds condenses to a cubic crystal for $\Gamma \gg 1$, while that with finitely extensible bonds remains in an imperfectly ordered glass structure. Non-neutral polyampholyte whose charge offset exceeds $\frac{1}{2}N^{1/2}$ behaves as polyelectrolyte: it consists of nonoverlapped chains for $\Gamma > 1$, and shrinks to the noncharged polymer regime for $\Gamma < 1$ (N is the number of charged monomers). Condensed counterions on polyampholyte screen the electric field, making non-neutral polyampholyte close to the neutral one. Added salt of comparable charge density as that of the polyampholyte further compactifies it. However, the addition of more salt results in the weakening of the polyampholyte nature and reentrant swelling of non-neutral polyampholyte.

PACS number(s): 61.25.Hq, 36.20.Ey, 64.60.Cn, 52.25.Wz

I. INTRODUCTION

Condensation and swelling driven by changes in temperature and ionic strength are important subjects for multichain polyampholytes, which are heterogeneous polymers consisting of linked monomers of both positive and negative charges [1]. Since polyampholytes show a strong tendency of self-neutralization without the help of counterions unlike polyelectrolytes, they will provide much physically interesting information and applications, including thermodynamical and dynamical properties, internal structure of globules, their stability, and phase transition between liquid and crystal states. These evidences will clarify the roles of the long-range Coulombic interactions in a constrained heterogeneous charged system of three dimensions.

For the case of polyampholytes with movable positive and negative monomers, the Coulombic interactions exert both repulsive and attractive forces of the same order. The former arises from unbalanced charges, and is predominant for strongly non-neutral polyampholytes, which are close to polyelectrolytes of one or the other sign. The latter arises from biased charge density fluctuations due to the formation of charge complexes of positive and negative monomers. Resultant interactions between oppositely charged segments of polyampholyte are attractive. The statistical properties of the single-chain polyampholytes were studied in the framework of the Debye-Hückel theory [2], and the Flory-type free-energy theory [3]. The importance of multichain effects and the occurrence of precipitation due to the pairing of oppositely charged chains in the semidilute and dense regimes of polyampholyte solution were pointed out, which showed limitation of the single-chain theories in realistic applications [4].

An early numerical study of single-chain polyampholytes was performed by the Monte Carlo simulations on a lattice model [5]. It found a collapsed globule for neutral polyam-

pholytes and a self-avoiding stretched coil for strongly non-neutral polyampholytes. In our earlier works [6,7], statistical and dynamical properties of polyampholytes for both the single-chain [6] and multichain [7] cases were investigated with the molecular dynamics simulations in the full three-dimensional space (nonlattice model). Another molecular dynamics simulation was done to examine the effect of applied electric field on the stretching behavior of single-chain polyampholyte [8].

In the previous studies of polyampholytes by molecular dynamics simulation [6,7], a very compact and dense globular state was discovered for the nonlattice model. It was shown that the attractive nature of the Coulomb forces for the globally neutral polyampholyte originates from the formation of complexes of positive and negative monomers (chains). A multichain polyampholyte showed a generally larger degree of compaction than its single-chain counterpart because of the creation of large void space among the chains [7]. For the neutral multichain system in a salt-free solution, thermodynamic stability of the globule at low temperatures against thermal agitations was proven numerically and theoretically. Also, salt ions were demonstrated to disintegrate a collapsed globule of neutral polyampholyte by migrating inside and screening the electric field; such dynamical processes, including oscillations of the volume and relaxation time, were so far adequately studied only by molecular dynamics simulations [7].

Experimentally, the swelling behavior of polyampholyte polymers and gels was studied by changing the salt concentration over several orders of magnitude at fixed temperature [9–11]. There it was shown that globally neutral polyampholytes occupy small volumes at low salt concentration, and swell monotonically with the addition of salt. By contrast, non-neutral polyampholytes are swollen at low salt concentration, and they shrink to the same volume as that of the neutral ones at high salt concentration.

The condensation and phase transition of a giant charged

particle system were studied for dusty plasmas [12–14], ionic colloids [15,16], and polyelectrolytes with counterions [17,18]. In the two-dimensional geometry, a plasma crystal having Wigner-Seitz cells was obtained at a large Coulomb coupling parameter. The three-dimensional studies of ionic colloids obtained the phase diagram of liquid and cubic crystals of the bcc, fcc, and hpc types depending on the conditions and parameters. The low-temperature behavior of non-neutral polyampholytes was previously studied by the Monte Carlo simulations [5]. These simulations considered only single-chain cases and adopted the lattice model, which becomes inaccurate due to the restricted number of neighboring sites at low temperatures. For this reason, numerical studies with the use of the off-lattice model are appropriate, as in the Monte Carlo and molecular dynamics studies of the strongly coupled systems [12,14,16–18].

The screening role of counterions and salt may be guessed by the case of dilute electrolytes at rather high temperature. The electrostatic potential may be approximated by the Yukawa potential $\varphi \sim (1/r)\exp(-r/\lambda_s)$. Here, $\lambda_s(n_s) = [\epsilon k_B T / 4\pi e^2 (Z_s^2 n_s + Z^2 n_0)]^{1/2}$ is the Debye screening length in the presence of counterions and salt ions, ϵ the dielectric constant of the solvent, k_B the Boltzmann constant, T the temperature, e the unit charge, n_s and Z_s the number density and valence of salt ions, and n_0 and Z the number density and valence of polyampholyte. (However, the Debye-Hückel theory without charge correlation effects is not applicable to dense, low-temperature electrolytes [18], as will be mentioned in Sec. IV B). This reduces the electrostatic energy by a factor $(\lambda_s/\lambda_D)^2 \sim 1/(1 + Z_s^2 n_s / Z^2 n_0)$, where $\lambda_D = \lambda_s(0)$. The Coulomb coupling parameter, which is the ratio of the electrostatic energy to thermal energy,

$$\Gamma = Z^2 e^2 / \epsilon a k_B T, \quad (1)$$

is modified as $\Gamma_s \sim \Gamma (\lambda_s/\lambda_D)^2 = (\lambda_B/a) (\lambda_s/\lambda_D)^2 \propto 1/Z_s^2 n_s T$. Here, a is the unit length (usually the exclusion radius of monomers), and $\lambda_B = \Gamma a$ is the Bjerrum length. The Coulomb coupling parameter Γ is the most relevant parameter to quantify the Coulombic interactions in charged systems [6]. We should note that the large value Γ arises from the large value Ze , the small value of ϵT , or both.

In this paper we will study the behavior of randomly charged *multichain* polyampholytes in the three-dimensional volume, with the use of molecular dynamics simulations. We will focus on the structure changes due to the Coulomb coupling parameter Γ (or the Bjerrum length λ_B), and the effect of counterions and added salt. We will show in Secs. III and IV that, by increasing the Coulomb coupling parameter (or by decreasing temperature), a globally charge-neutral polyampholyte collapses monotonically to a compact globule, in which chains interpenetrate with each other and reptate around the whole volume of the globule. For $\Gamma \gg 1$, it condenses into an ordered cubic crystal when the connecting bonds are widely extensible. For the more realistic case of finitely extensible bonds, we obtain a glassy globule with an imperfectly ordered structure, which retains substantial frustrations. The multichain effect is found to cause much larger volume changes of polyampholytes than the single-chain effect does.

Also, the behavior of non-neutral polyampholytes with and without salt and counterions is studied. Even a non-neutral polyampholyte forms charge complexes (or clumps [4]) if the global charge offset is less than $N^{1/2}$. Otherwise, it is swollen at $\Gamma \gg 1$ due to Coulombic repulsions, which shrinks monotonically to the volume similar to that of the noncharged polymers at $\Gamma \sim 1$. The volumetric changes of slightly non-neutral polyampholytes are reentrant, first shrinking and then swelling with the change in the Coulomb coupling parameter. A polarized cloud of coexisting counterions is shown to surround and neutralize unbalanced charges of polyampholyte, which screens the electric field. However, the polyampholyte chains remain separated at all values of the coupling parameter. In the presence of counterions and salt whose charge density is comparable to that of polyampholyte, the non-neutral polyampholyte is more compact than in the salt-free solution, i.e., when it is screened by counterions only. For $\Gamma \gg 1$, all the chains aggregate together. At fixed value of the coupling parameter, on the other hand, the volume of highly non-neutral polyampholyte changes in a reentrant fashion with the salt ionic strength.

We would like to make some remarks about the word “temperature” and its relation with the Coulomb coupling parameter. We note that the more general parameter is the Coulomb coupling parameter rather than temperature. In real experiments, it is not possible to change the temperature over a wide range for a single polyampholyte, since the solvent may freeze or vaporize beyond certain temperatures. Nonetheless, there is more than one way to change the Coulomb coupling parameter $\Gamma = e^2 Z^2 / \epsilon a k_B T$, either by using polyampholytes that are comprised of monomers of different valence Z or a solvent of other dielectric constants ϵ . Thus, we can have access to different regimes of $\Gamma = T_0/T$ in separate experiments, where

$$T_0 = Z^2 e^2 / \epsilon a k_B \quad (2)$$

is the base temperature at which the electrostatic energy at the distance a is equal to thermal energy. The base temperature is higher for larger valence Z or smaller dielectric constant ϵ . In numerical simulations, a wide range of the Coulomb coupling parameter is accessible in terms of sequential temperature changes for one specific polyampholyte. Second, the functional dependences to be shown in Secs. III and IV are considered to be equilibrium ones. During the gradual temperature change of three orders of magnitude, the equations of motion are integrated for 2 000 000 MD (molecular dynamics) steps.

This paper will be organized as follows. In Sec. II of this paper the equations of motion, adopted parameters, and the definitions of observed quantities are presented. Condensation of globally neutral polyampholytes at low temperatures ($\Gamma \gg 1$) is shown in Sec. III. The swelling behavior of non-neutral polyampholytes in the presence and absence of counterions and added salt is described in Sec. IV. Section V will summarize the results of this paper.

II. THE EQUATIONS OF MOTION AND SIMULATION PARAMETERS

The multichain polyampholytes adopted in this study consist of six 32-mer chains. The initial configurations of the

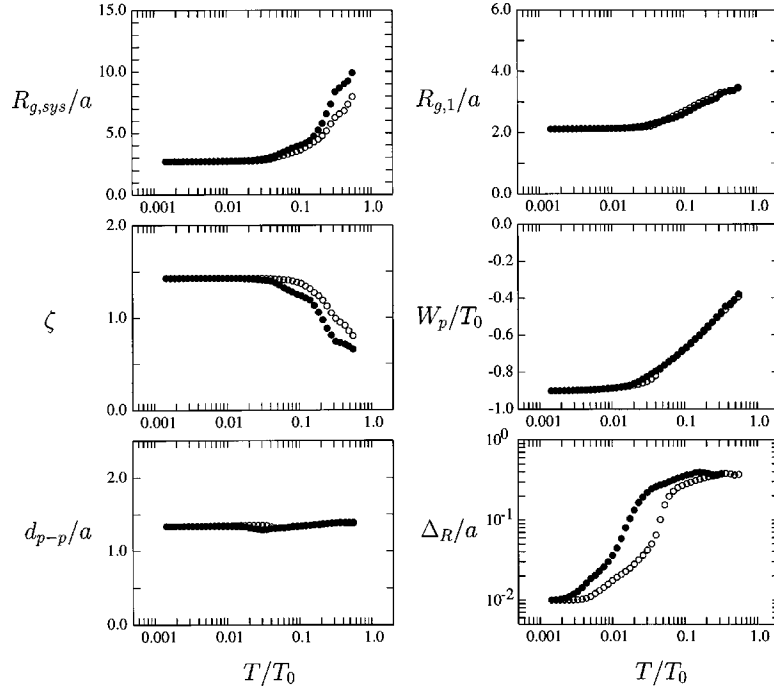


FIG. 1. The temperature dependence of globally neutral polyampholyte with widely extensible bonds (six 32-mers) is shown for the cooling and heating stages with closed and open circles, respectively (an average of 15 runs of different random sequences). The shown quantities are the system gyration radius of all the monomers $R_{g,sys}$, the single-chain gyration radius $R_{g,1}$, the filling index that indicates chain overlapping $\zeta = N_c^{1/3} R_{g,1}/R_{g,sys}$, the electrostatic energy W_p , the connected monomer distance d_{p-p} , and time fluctuations of monomer distances Δ_R ; T_0 is the base temperature at which the electrostatic and thermal energies become equal.

perature becomes $T_0 \cong 700Z^2$ (K). Since we use the time step $\Delta t = 0.01\omega_p^{-1}$, then, in one time interval τ_0 , 200 000 integration steps are executed.

The boundary conditions of an isolated charge system are used in this study. The normal to the wall velocity of the monomers hitting a boundary sphere, which is located at the radius $r = 21a$, is inverted in an elastic fashion. The choice of such boundary conditions is justified for studies of physics processes, since it was confirmed in our previous study with the periodic boundary conditions (the particle-mesh Ewald algorithm [19,20]) that the swelling behavior of polyampholytes is only slightly modified compared to those for the isolated system [21].

In order to quantify the swelling of polyampholytes, we measure the gyration radius of the system (all chains) by

$$R_{g,sys} = \left(\frac{1}{N} \sum_{j=1}^N (\mathbf{r}_j - \langle \mathbf{r} \rangle)^2 \right)^{1/2}, \quad (7)$$

where \mathbf{r}_j is the coordinate of the j th particle, $\langle \mathbf{r} \rangle$ is the mass center of monomers, and N is the number of the monomers of polyampholyte. The gyration radius of a single chain $R_{g,1}$ is defined by averaging the gyration radii of N_c chains. We define the filling index by

$$\zeta = N_c^{1/3} R_{g,1} / R_{g,sys}. \quad (8)$$

The criterion $\zeta \geq 1$ is an index for that the chains are overlapped and forming a globule; for $\zeta < 1$ the chains are scattered across the domain. We also measure the average distance of connected monomers d_{p-p} , the electrostatic energy

$$W_p = \frac{1}{N} \sum_i \sum_{j>i} Z_i Z_j e^2 / \epsilon |\mathbf{r}_i - \mathbf{r}_j|, \quad (9)$$

and the time fluctuations of the monomer distances,

$$\Delta_R = \left[\frac{2}{N(N-1)} \sum_i \sum_{j>i} \left(\frac{\langle r_{ij}^2 \rangle - \langle r_{ij} \rangle^2}{R_{g,sys}^2} \right) \right]^{1/2}, \quad (10)$$

where $r_{ij} = |\mathbf{r}_i - \mathbf{r}_j|$ and $\langle r_{ij} \rangle$ is a short-time average of r_{ij} .

In the following figures, viz., Figs. 1, 3, 7, 8, 9, and 11, the abscissas are labeled by T/T_0 , which is exactly the inverse of the Coulomb coupling parameter Γ , i.e., $T/T_0 = \Gamma^{-1}$. (In Secs. III and IV, results are shown in the energy unit where the temperature T should be read as $k_B T$.) As remarked above, although the dependences of the physical quantities are obtained by gradual and sequential changes in temperature, such dependences can be regarded as equilibrium ones.

III. SWELLING BEHAVIOR OF NEUTRAL POLYAMPHOLYTES

A. General temperature dependences

The dependence of globally charge-neutral polyampholyte on temperature (inverse of the Coulomb coupling parameter) is shown in Fig. 1. Six quantities in the figure are the system gyration radius of all the chains that represents the multichain effects $R_{g,sys}$, the single-chain gyration radius $R_{g,1}$, the filling index that indicates chain overlapping ζ , the electrostatic energy W_p , the average distance of connected monomers d_{p-p} , and the fluctuations of (all) the monomer

distances Δ_R . Equations (7)–(10) are the definitions of these quantities. The filled and open circles correspond to values in the cooling and heating stages, respectively.

First, we state that energy equipartition is established between kinetic and elastic energies of the polyampholyte, $W_{\text{kin}} \cong W_{\text{spr}} \cong \frac{3}{2}T$, during the temperature changes. For the neutral polyampholyte, both the gyration radii $R_{g,1}$ and $R_{g,\text{sys}}$ decrease monotonically with a decrease in temperature. A globule is formed ($\zeta \geq 1$) at $T/T_0 \sim 0.2$ at which the radius of the polyampholyte becomes comparable to the Bjerrum length, $R_{g,\text{sys}} \sim \lambda_B$. The macroscopic quantities such as the gyration radii become insensitive to temperature for $T/T_0 \leq 0.03$, which implies that the globule is approaching the highest density state allowed to the system. The observation that the single-chain gyration radius becomes close to the system gyration radius $R_{g,1} \sim R_{g,\text{sys}}$ is remarkable, since it indicates that the chains in the globule penetrate with each other and reptate through the whole globule. This is entirely consistent with the physical idea that a clump of several chains can be viewed as a little piece of concentrated polymer solution [22].

The change in the system gyration radius in Fig. 1 is twice as large as that in the single-chain gyration radius. Therefore, in terms of the volume, the multichain effect mostly prevails over the single-chain effect [7]. It is noted that the path of the system gyration radius for the cooling stage is slightly higher than that of the heating stage at high temperatures $T/T_0 > 0.1$. Close inspection shows that the heating paths of many polyampholytes with different sequences almost overlap (open circles), which constitute the lower envelope of the cooling paths (solid circles) that deviate in the above temperature range (average values over different sequences are depicted). We consider that the smaller system gyration radius of polyampholytes in the heating stage manifests the dominance of attractive Coulomb forces between the oppositely charged complexes residing within the medium scale length $r < \lambda_B$. (This point will be again considered in Fig. 3.) For the case of polyelectrolytes, the attractive Coulomb forces were shown to appear by mediation of counterions [17,23].

The fluctuations of the monomer distances Δ_R decrease rapidly with a decrease in temperature. In the intermediate temperature range $0.008 < T/T_0 < 0.03$, it changes approximately linearly in temperature. At very low temperatures $T/T_0 \leq 0.008$, the fluctuations of the monomer distances scale as $\Delta_R \sim T^{1/2}$, which correspond to thermally driven harmonic oscillations of the monomers. Its fluctuations at $T/T_0 \sim 0.001$ are reduced to a few percent that of adjacent monomers.

The sign of the electrostatic energy is always negative for polyampholytes, indicating again the dominance of attractive Coulomb forces over repulsive ones. Accordingly, the average electrostatic energy, to which the closest pairs of unlike-sign charges make the largest contributions, becomes more negative with a decrease in temperature, as almost inversely proportional to $3/2$ power of the gyration radius of each chain [3,22], $|W_p| \sim R_{g,1}^{-3/2}$. The relation $W_p/T_0 \geq -1$ for the condensed globule at low temperatures well corresponds to the close packing of monomers $r \cong a_{\text{LJ}}$.

It is quite instructive to mention that, even if the bonds between monomers are removed (cut), the collapsed globule

at low temperatures $T/T_0 < 0.01$ is not modified. The condensed globule stays in a stable state under the Coulomb forces. As one expects, the chain connection makes for the condensation of polyampholyte under the conditions at which a neutral charged particle system (plasma) of the same density does not condense at all. Indeed, the same density plasma as the above polyampholyte, which also represents a dilute solution of Na^+ and Cl^- , becomes “gas,” become condensed in a similar time scale as the polyampholyte, if the size of the simulation domain is cut in half, i.e., eight times in density.

B. Condensation to crystals

We first describe physically interesting cases of the spring-beads model of a purely entropic nature. These cases serve as the baseline for the more realistic cases with finitely extensible bonds which will be treated later in this section. Figure 2 depicts the bird’s-eye view plots and the pair correlation functions of neutral polyampholyte at various temperatures. The pair correlation function $G_{++}(r)$ is for the monomer pairs of equal signs, and $G_{+-}(r)$ for those of the opposite signs. The scattered chains are seen to get close and condensed with a decrease in temperature, as we proceed from (a) to (c). The discrete structure becomes evident in the pair correlation functions at low temperatures $T/T_0 < 0.01$ ($\Gamma > 100$). Namely, the polyampholyte at the temperature $T/T_0 \sim 1/85$ is only partially ordered, whereas a spatially ordered structure appears at the low temperature $T/T_0 \sim 1/170$. The profiles of the pair correlation functions are close among different runs, which shows the establishment of equilibrium. The first peak of the G_{+-} function is always inside that of G_{++} . This indicates the formation of complexes of positive and negative charges, which is attributed to the attractive Coulomb forces.

A quantitative analysis of the globule of Fig. 2(c) shows that the first and second peaks of the G_{+-} function are located at $r \cong 1.07a$ and $2.10a$, respectively. The position of the first peak is about 5% less than the effective exclusion radius $d_{+-}^{(1)} = 2^{1/6}a_{\text{LJ}} \cong 1.12a$. For the bcc crystal, the positions of the first peaks of G_{+-} and G_{++} should satisfy $d_{+-}^{(1)}/d_{++}^{(1)} = 2/\sqrt{3} \cong 1.15$, and the first and second peaks of G_{+-} should be $d_{+-}^{(2)}/d_{+-}^{(1)} = (11/3)^{1/2} \cong 1.91$. These relations are well satisfied by the polyampholyte crystal observed in Fig. 2(c). The number of monomers contained in the first and second peaks of G_{+-} , averaged for the core monomers (less than $1.5a_{\text{LJ}}$ from the gravity center) of 20 condensed globules of different sequences, is 7.9 and 23.3, respectively. For the bcc crystal, they should be 8 and 24, respectively. All this information proves the formation of the cubic crystal of the bcc type. This will be confirmed later in Fig. 5(a).

From Figs. 2(b) and 2(c) we infer that phase transition from the glass to crystal states occurs between the temperatures corresponding to these panels, namely at $T/T_0 \cong 8 \times 10^{-3}$ ($\Gamma \sim 130$). At this temperature, the slope of time fluctuations of monomer distances Δ_R changes discontinuously. This transition temperature is approximately of the same order as other strongly coupled systems [12,15,16].

Next, different cases of *finitely extensible bonds* with impenetrable monomers are examined. So far for the cases shown in Figs. 1 and 2, the elastic energy $3T/a^2$ became small in comparison with the Coulomb energy, which re-

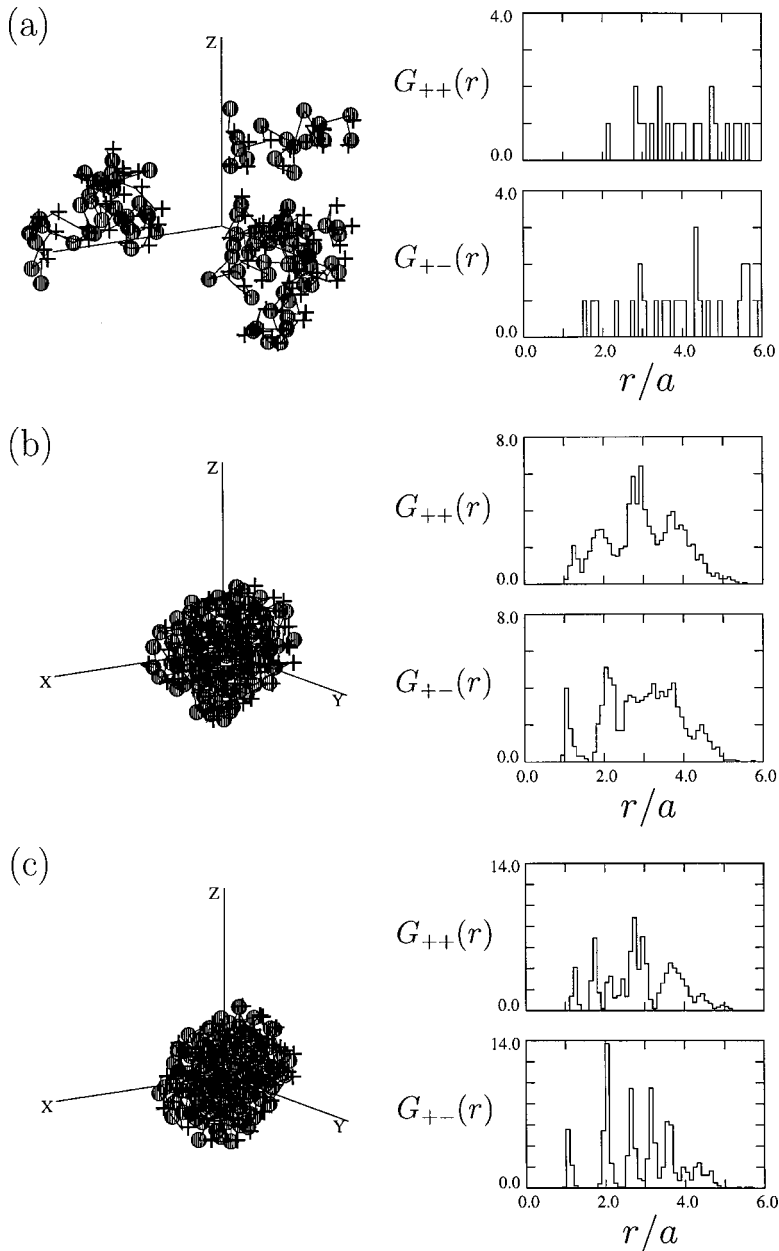


FIG. 2. The bird's-eye view plots (left) and the pair correlation functions (right) for the neutral polyampholyte with widely extensible bonds are shown for the temperatures (a) $T/T_0 \cong 1/5$, (b) $1/85$, and (c) $1/170$. The $+$ and \bullet symbols represent positive and negative monomers, respectively, and $G_{++}(r)$ and $G_{+-}(r)$ are the pair correlation functions for the monomer pairs of equal-sign and opposite-sign charges, respectively.

sulted in a complete reordering of charged monomers driven by Coulomb interactions. To see the effect of finitely extensible bonds, other runs are described below in which the largest distance between connected monomers is limited by the length a_{\max} : $|\mathbf{r}_i - \mathbf{r}_{i+1}| < a_{\max}$. This is realized by providing a high bond potential $U(r)$ for $r \geq a_{\max}$.

Simulation results for the globally neutral polyampholyte with finitely extensible bonds $a_{\max} = 1.4a$ (six 32-mers) are shown in Fig. 3. The overall dependences on temperature are similar to those of widely extensible bonds in Fig. 1. However, quantitative differences are present. The average bond length d_{p-p} is smaller and the electrostatic energy is less negative than that in Fig. 1. On the contrary, the system gyration radius of the polyampholyte with finitely extensible bonds is generally larger than that with widely extensible bonds, except at low temperatures. Especially, the difference of the curves of Figs. 1 and 3 for the heating stage at temperatures $T/T_0 > 0.3$ should be remarked, when the chains start to be separated. For the case of finitely extensible

bonds, the Coulomb attractive forces are considered to be a little weaker because charge fluctuations are canceled more locally by neighboring monomers due to the bond constraint. This is analogous to a lesser degree of compaction for multichain polyampholyte with alternate sequences [7]. These observations again support that uncompensated charge fluctuations inherent from charge sequences promote compaction of polyampholytes.

An imperfectly ordered structure is seen in the pair correlation functions of the above polyampholyte. Separated peaks in the $G_{+-}(r)$ function, which are not present in Fig. 4(a), first appear at the temperature $T/T_0 \sim 1/40$. They do not undergo significant changes with a decrease in temperature, unlike the phase transition for the polyampholyte with widely extensible bonds. The peaks seen at the very low temperature $T/T_0 \sim 1/340$ of Fig. 4(b) are located at similar positions as those of Fig. 2(c), but are markedly broad and not well separated except for the first peak of the $G_{+-}(r)$ function at $r \cong a_{LJ}$. The number of monomers contained

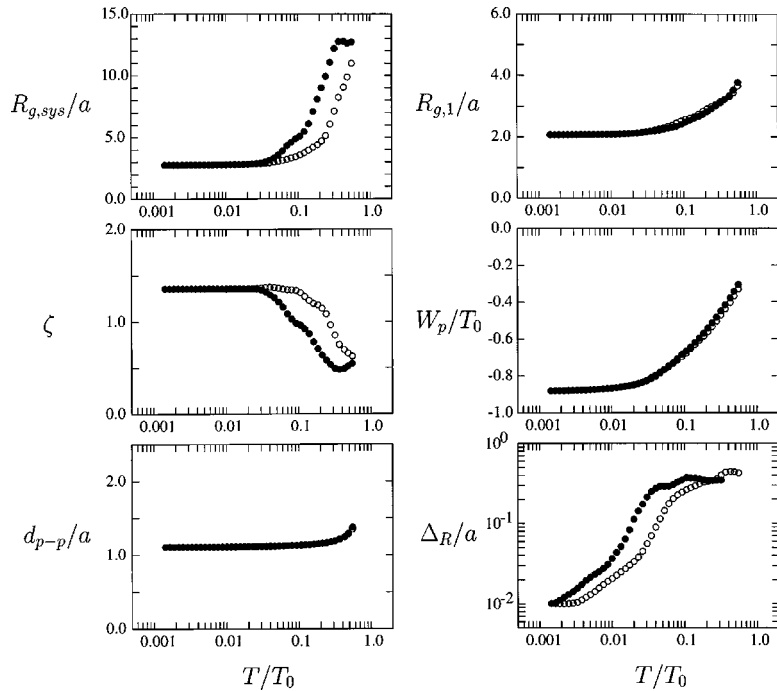


FIG. 3. The temperature dependence of globally neutral polyampholyte with finitely extensible bonds (six 32-mers) is shown; the bond lengths are limited as $|\mathbf{r}_i - \mathbf{r}_{i+1}| \leq 1.4a$. The plot format is the same as for Fig. 1, and the data are an average over runs of different random sequences.

there is 6.2 on average, which is less than eight of the bcc crystals. Although we find the tendencies toward crystallization, the absence of a repeated structure of large scales defines it as a glass.

The bird's-eye views of Fig. 5(a) show a structure observed for the neutral polyampholyte with widely extensible bonds at the temperature $T/T_0 \sim 1/340$. The left and middle columns depict, respectively, the polymer chains and monomers of the condensed globule. The right column depicts the

monomers in the cross-sectional layer of width $2a/\sqrt{3}$ that contains the center of the globule. Red and green spheres represent the positively and negatively charged monomers, respectively. A high degree of the chain reptation through the whole globule is seen, in which different chains include each other. The condensed globule exhibits an ordered structure of a square shape, where the positive and negative monomers are placed in an alternate chess-board fashion. Sequential plots of thin cross sections show that the positive

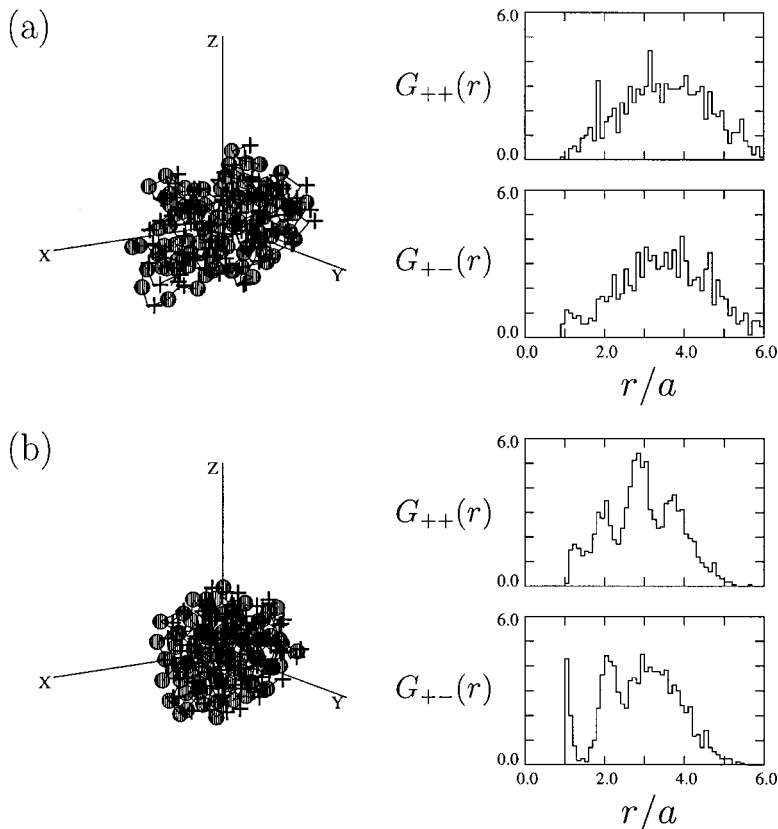


FIG. 4. The bird's-eye view plots (left) and the pair correlation functions (right) for the polyampholyte with finitely extensible bonds, at the temperatures (a) $T/T_0 \cong 1/21$ and (b) $1/340$. The $G_{++}(r)$ and $G_{+-}(r)$ pair correlation functions are for the pairs of equal-sign and opposite-sign charges, respectively.

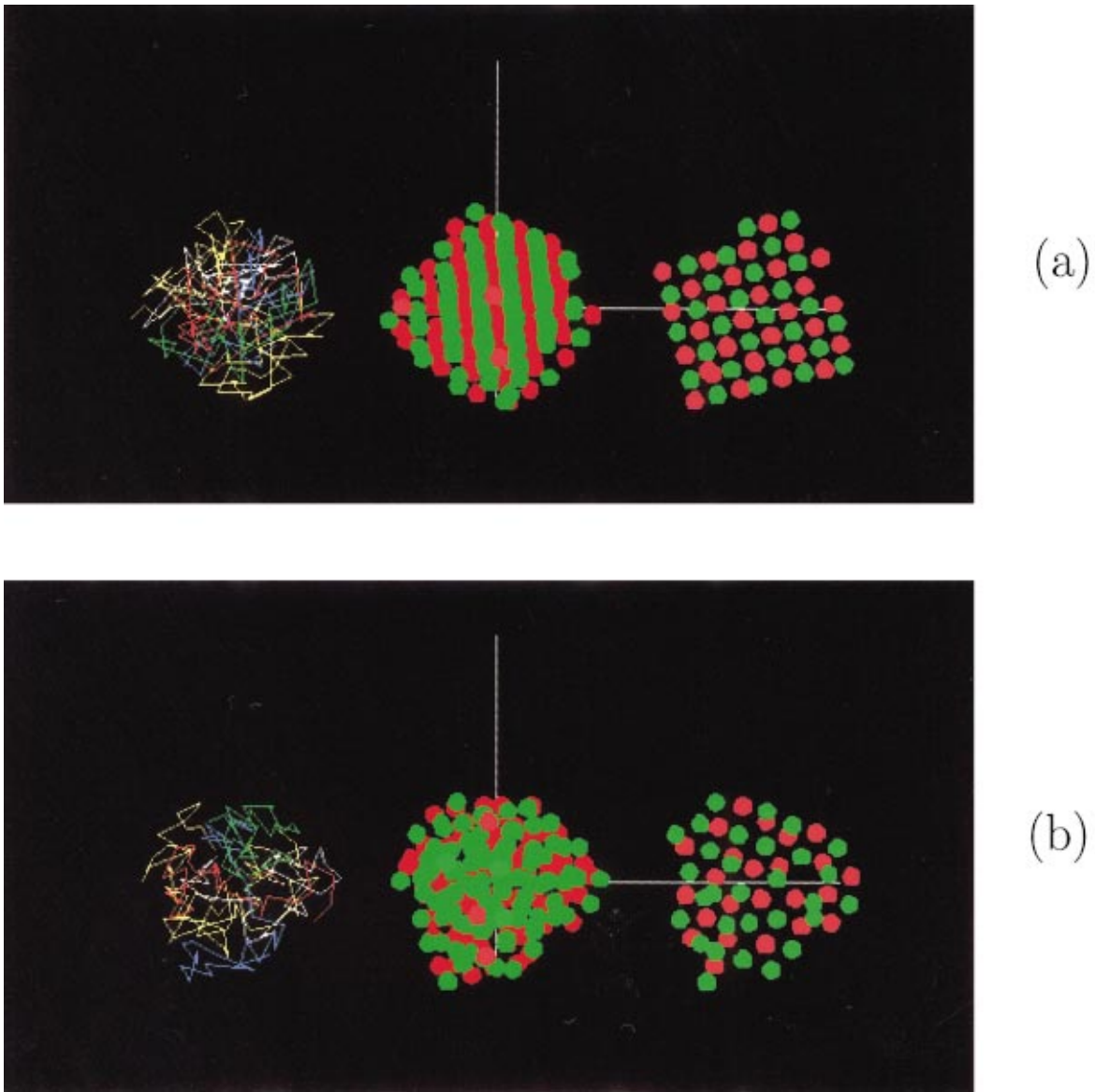


FIG. 5. (color) The bird's-eye views of (six) chains and corresponding monomers of a condensed globule, and the monomers in the middle cross section (from left to right) are depicted for (a) the globally neutral polyampholyte with widely extensible bonds, and (b) that with finitely extensible bonds, both at the temperature $T/T_0 \cong 1/340$. The chains in the left column are color coded (yellow color appears twice), and the monomers with positive and negative charges are shown with red and green sphere, respectively.

and negative monomers are located on different planes that are separated by approximately $1.2a (\cong 2a/\sqrt{3})$. This information along with that of the pair correlation functions in Fig. 2 confirms that the observed globule has the structure of the bcc crystal.

For the polyampholyte with finitely extensible bonds in Fig. 5(b), the tendencies toward an ordered structure are hindered by the bond constraint. The monomers are ordered in a short scale, with one monomer surrounded by approximately six monomers. But, two monomers of equal-sign charge frequently reside at neighboring positions at which the opposite-sign monomer is expected for the crystal of Fig. 5(a). Thus, the observed structure is deformed from a cubic one. Since the chains repel each other by the volume exclusion of the monomers on them, the polymer chains tend to make their own blobs and exclude the others, except for penetration of stretched segments. The globule here includes significant amount of frustrations, and is above the global

energy minimum, as is reflected in less negative electrostatic energy in Fig. 3 than for the polyampholyte with widely extensible bonds.

IV. SWELLING BEHAVIOR OF NON-NEUTRAL POLYAMPHOLYTES

The effects of unbalanced charges on polyampholytes are examined in this section. The number of chains and monomers per chain is $N_c = 6$ and $N_1 = 32$, respectively; the number of monomers in one polyampholyte is $N = N_c N_1 = 192$. The charge signs of the monomers are chosen randomly. Thus, each chain has basically a net charge δQ_α ($\alpha = 1 \sim N_c$), and the amount of global charge offset per polyampholyte is $\delta Q = \sum_{\alpha=1}^{N_c} \delta Q_\alpha \sim \pm e\sqrt{N}$ on average. The behavior of non-neutral polyampholytes in the presence of counterions and salt is examined in Secs. IV B and IV C.

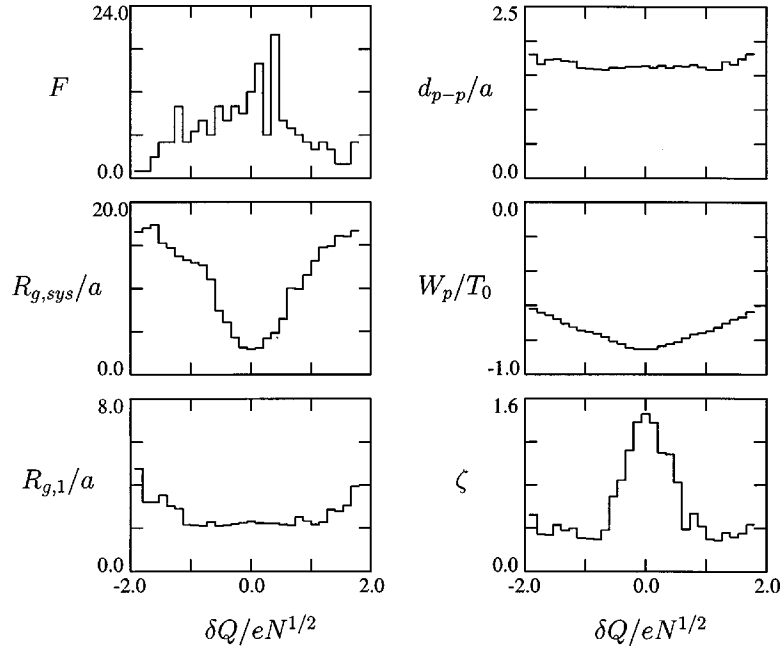


FIG. 6. The effect of globally uncompensated charges is depicted for the group of 180 non-neutral, six 32-mer polyampholytes of random sequences. The probability F of having global charge offset δQ (normalized by $eN^{1/2}$), the system gyration radius $R_{g,sys}$, the single-chain gyration radius $R_{g,1}$, the average distance between connected monomers d_{p-p} , the electrostatic energy W_p , and the filling index $\zeta = N_c R_{g,1}/R_{g,sys}$ are shown against charge offsets, at the temperature $T/T_0 \sim 1/430$.

A. Polyampholytes without counterions

A large number (180) of polyampholytes having random charge sequences and different initial conformations are generated. The left column of Fig. 6 shows, from top to bottom, the probability F of the polyampholytes having the global charge offset δQ which is nearly Gaussian centered at $\delta Q = 0$, the system gyration radius $R_{g,sys}$, and the single-chain gyration radius $R_{g,1}$. The charge offset in the abscissas is normalized by the critical charge offset $Q_c = eN^{1/2}$. In the right column, the bond-connected monomer distance d_{p-p} , the electrostatic energy W_p , and the filling index ζ are shown.

The gyration radii take small values for the null global charge offset, and they increase with the charge offset. The system gyration radius $R_{g,sys}$ increases rapidly at the charge offset $|\delta Q|/Q_c \sim 0.5$, while individual chains begin to stretch for larger charge offsets. This again reveals that the multi-chain effect dominates in magnitude over the single-chain effect when temperature (the Coulomb coupling parameter) changes. In simpler words, the clump of several chains swells more because chains move a little further away from each other, while parts of the same chain shift much less.

The observation that the filling index becomes larger than unity, $\zeta \geq 1$, for the polyampholytes with

$$|\delta Q|/eN^{1/2} \leq 1/2, \quad (11)$$

indicates that charge complexes (or clumps) are formed only for nearly neutral polyampholytes whose charge offset satisfies Eq. (11). Otherwise, the charge complexes are disintegrated, and the polyampholyte consists of nonoverlapped scattered chains. This situation is consistent with the theoretical analysis of Everaers, Johner, and Joanny [4], showing that pairing of chains occurs most efficiently under the con-

dition of Eq. (11), where chains in the distribution tail are oppositely charged with respect to majority of the chains (the width of the chain distribution F is approximately $eN^{1/2}$).

Figure 7 depicts the typical dependence of non-neutral polyampholytes against temperature $T/T_0 = \Gamma^{-1}$, which are sampled from the runs in Fig. 6. The global charge offsets δQ for these runs are $|\delta Q|/eN^{1/2} = 0.0, 0.72, 0.87, 1.15,$ and 1.73 . By the $\zeta \geq 1$ criterion, we find that a complex of chains (globule) is formed for the neutral polyampholyte (filled circles) at low temperatures $T/T_0 < 0.3$ (the Bjerrum length $\lambda_B > 3a$); oppositely charged chains attract each other. The system gyration radius increases monotonically with an increase in temperature, and reaches the thermal state at $T/T_0 \sim 1$ in which the Coulomb forces play little role. This is the so-called *polyampholyte regime* [10,11].

For the very non-neutral case with $|\delta Q|/eN^{1/2} = 1.73$ (square symbols), the chains tend to take the largest distance at low temperatures due to electrostatic repulsions between excess charges. At high temperatures, since the Coulomb forces become less important, the chains come closer and the system gyration radius is reduced to that of the aforementioned thermal state. The chains of non-neutral polyampholyte whose charge offset does not satisfy Eq. (11) are separated at all temperatures (*the polyelectrolyte regime*). The electrostatic energy becomes systematically less negative for larger charge offset, indicating less attractive nature of the Coulombic interactions.

It is interesting that the temperature dependence of the system gyration radius for the polyampholyte with medium charge offset $|\delta Q|/eN^{1/2} = 0.5 \sim 1$ becomes reentrant in Fig. 7. The minimum radius occurs at an intermediate temperature T_m , where attractive Coulomb forces slightly overcomes repulsive ones. The temperature T_m shifts to the higher side when the charge offset becomes larger, since

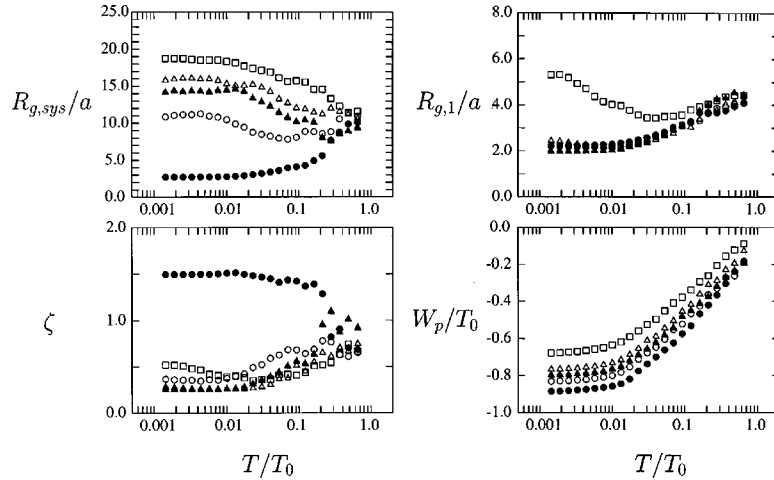


FIG. 7. The typical behavior of globally non-neutral polyampholytes against temperature (the heating stage) is shown: the system gyration radius $R_{g,sys}$, the single-chain gyration radius $R_{g,1}$, the filling index $\zeta = N_c^{1/3} R_{g,1} / R_{g,sys}$, and the electrostatic energy W_p . The global charge offsets shown by filled and open circles, filled and open triangles, and squares are $|\delta Q|/eN^{1/2} = 0.0, 0.72, 0.87, 1.15,$ and 1.73 , respectively.

excess charge intensifies the repulsive forces and broadens the polyelectrolyte regime. The single-chain gyration radius $R_{g,1}$ behaves somewhat differently. For small charge offsets, the radius increases monotonically with temperature. Only for large charge offsets $|\delta Q|/eN^{1/2} \geq 1.5$, the gyration radius of individual chains becomes reentrant. This change is mostly attributed to the increase in the distance of the connected monomers d_{p-p} , which is suppressed in ordinary polyampholytes with finitely extensible bonds.

The variance of the system gyration radius among the polyampholytes having the same global charge offset but different sequences is depicted in Fig. 8. For either highly non-neutral or nearly neutral polyampholytes in Figs. 8(a) and 8(c), the trends of the system gyration radius against temperature are similar among those with the same charge offset, and their variances are rather small. However, large variance occurs for the polyampholytes with medium charge offsets $|\delta Q|/eN^{1/2} \sim 1/2$ in Fig. 8(b). This sequence sensitivity, where only one or two polyampholytes out of five are associated with the charge complex formation while others are dominated by separated chains or complexes, is observed for $|\delta Q|/eN^{1/2} = 0.4 \sim 0.8$. The sensitivity to the specific sequence might be of great potential importance in protein, and in biopolymer context in general.

B. The effect of counterions

Non-neutral polyampholytes of any realistic concentration in solution attract charge-neutralizing counterions, which form surrounding clouds. Here, we briefly study the effect of counterions and that of added salt on highly non-neutral polyampholytes whose global charge offset exceeds the critical charge offset $Q_c = eN^{1/2}$.

The non-neutral polyampholytes in Secs. IV B and IV C (six 32-mers, with finitely extensible bonds) consist of 30% positive monomers and 70% negative monomers ($N_+ = 58$, $N_- = 134$). The charged monomers are randomly distributed in a row onto six chains. The global charge offset is $\delta Q/Q_c = (N_+ - N_-)/N^{1/2} \sim -5.5$. We note that such highly non-neutral polyampholytes act as polyelectrolytes in the ab-

sence of counterions (cf. Fig. 7). The number of coexisting monovalent counterions is $N_{c+} = 76$, which exactly balances the excess charge of each polyampholyte.

Figure 9 shows the temperature dependence of the system gyration radius $R_{g,sys}$, the single-chain gyration radius $R_{g,1}$, the filling index ζ , and the electrostatic energy W_p . The four series of data points correspond to non-neutral polyam-

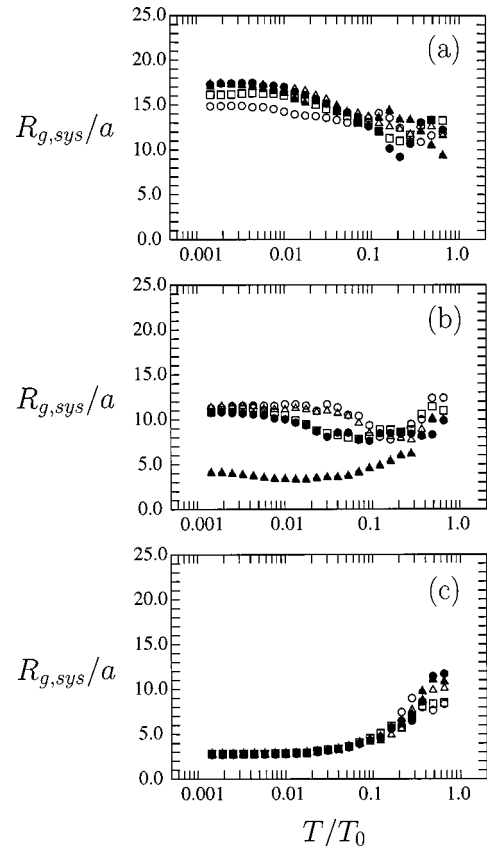


FIG. 8. The variance of the system gyration radius due to different charge sequences is depicted for the group of polyampholytes of Fig. 7. The polyampholytes in each panel have identical global charge offset, which is (a) $|\delta Q|/eN^{1/2} = 1.29$, (b) 0.72 , and (c) 0.14 .

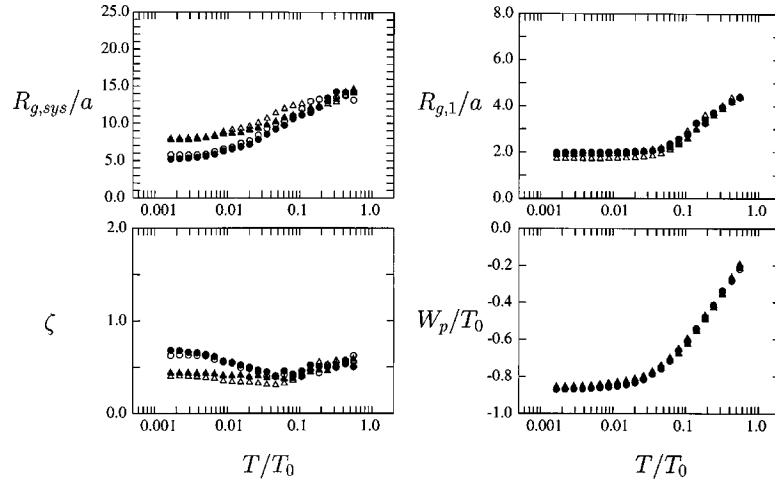


FIG. 9. The temperature dependence of non-neutral polyampholytes in the presence of counterions is shown for the six 32-mer polyampholytes with finitely extensible bonds. The four cases shown are different in random sequences. The global charge offset is $\delta Q/eN^{1/2} \sim -5.5$ ($N_+ = 58$, $N_- = 134$), and the positive counterions ($N_{c+} = 76$) exactly balance the offset charge. Depicted in the figure are the system gyration radius $R_{g,sys}$, the single-chain gyration radius $R_{g,1}$, the filling index $\zeta = N_c^{1/3} R_{g,1}/R_{g,sys}$, and the electrostatic energy W_p .

polyampholytes of different random sequences. Unlike the non-neutral polyampholytes without counterions in Sec. IV A, the system gyration radius now decreases monotonically with decrease in temperature. Its average values at medium and low temperatures $T/T_0 = 10^{-1} \sim 10^{-3}$ are a few times larger than their counterparts of the neutral polyampholytes. The filling index never exceeds unity at any temperatures, indicating that non-neutral polyampholytes with counterions alone consist of separated globules or chains.

The non-neutral polyampholyte with counterions is depicted by the bird's-eye view plot in the left column of Fig. 10. The chains are separated at the medium temperature $T/T_0 \sim 1/5$. About 80% of the counterions are condensed on

non-neutral sites of the polyampholyte, while the rest are floating in the space among the chains. The amount of non-condensed counterions is close to $N^{1/2}$, which means that approximately $eN^{1/2}$ bare charges remain on the polyampholyte [cf. Eq. (11)]. We note that the Debye length is written

$$\lambda_D/a = (aT/4\pi e^2)^{1/2} = (1/4\pi\Gamma)^{1/2}, \quad (12)$$

which falls within the exclusion radius except at high temperatures $T/T_0 \gg 1$ ($\Gamma \ll 1$). The above observation shows that the electric field is not screened at the Debye length. Therefore, the Debye-Hückel theory is not applicable to the

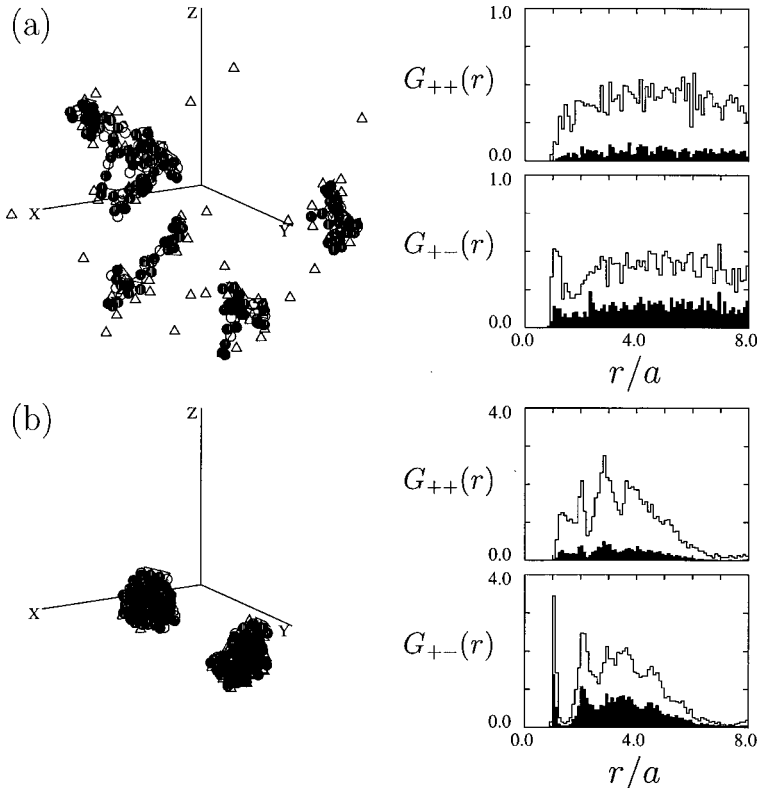


FIG. 10. The bird's-eye view plots (left) and the pair correlation functions (right) are shown for the non-neutral polyampholytes with counterions (Fig. 9) at the temperatures (a) $T/T_0 \cong 1/5$ and (b) $1/85$. The $G_{++}(r)$ and $G_{+-}(r)$ pair correlation functions are for the pairs of equal-sign and opposite-sign charges, respectively, and the shaded areas show the contribution of the counterions.

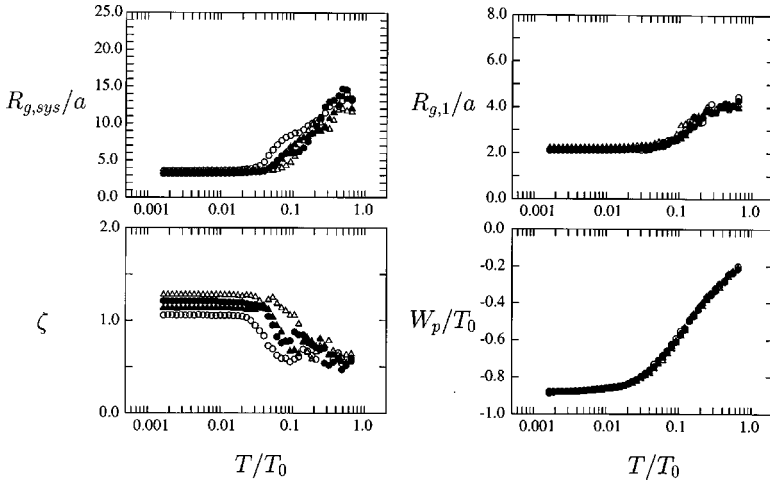


FIG. 11. The temperature dependence of non-neutral polyampholytes in the presence of both counterions and salt is shown. The parameters and conditions are the same as those of Fig. 9, except for the addition of salt ions ($N_{s+}=58$, $N_{s-}=58$, and $N_{c+}=76$). The charge content of salt and counterions equals that of the polyampholyte.

strongly coupled system with $\Gamma \geq 1$. At low temperatures $T/T_0 \leq 0.07$, counterions are absorbed by the globules. Even at the very low temperature $T/T_0 \sim 1 \times 10^{-3}$, the non-neutral polyampholyte with counterions alone stays in a multiglobular phase. This situation of redistribution of counterions between the globule interior and surrounding solution has recently been examined [24]. Our observations are in full qualitative agreement with their results.

The pair correlation functions in the right column of Fig. 10 show both the total number of monomers viewed from the monomers of polyampholyte and the contribution of the counterions (shaded areas). The negative monomers are more closely associated with positive ions (monomers and counterions) than with negative ones. At the low temperature depicted in the bottom panels of Fig. 10, a few globules are formed (typically, two for the six 32-mer case). All the counterions are now absorbed by the globules. The shaded areas of the pair correlation functions tell us that the counterions bound to the polyampholyte are not distinguishable from the bond-connected monomers.

C. The effect of added salt

The simulation settings here are the same as for Fig. 9, except for the addition of salt: the numbers of salt and (neutralizing) counterions are $N_{s+}=N_{s-}=58$ and $N_{c+}=76$, respectively. The total charge of these free ions is equal to that of the polyampholyte, $N=192$, whose global charge offset is $\delta Q/eN^{1/2} \sim -5.5$.

The screening effect of the electric field by added salt is more prominent than by counterions alone, as shown in Fig. 11. The system gyration radius now decreases with a decrease in temperature, like the neutral polyampholyte shown in Fig. 1. It is remarkable that the monoglobular phase is realized (i.e., $\zeta > 1$) at low temperatures $T/T_0 \leq 0.05$. There, the variance of the gyration radii among the runs of different charge sequences is small. The presence of salt makes non-neutral polyampholytes more compact than for counterions only. We note that the system gyration radius in Fig. 11 is approximately 1.3 times (or volume $\cong 2$ times) that of the neutral polyampholyte of Fig. 1, and that the total number of monomers in the former is exactly twice that of the polyampholyte of the latter. This implies that counterions and salt ions are absorbed by the globule as if they are the building

blocks of non-neutral polyampholyte. The observation that the system and individual gyration radii are comparable, $R_{g,sys} \sim R_{g,1}$, again shows high degree of chain reptation in the globule.

The non-neutral polyampholyte with salt at medium temperature is shown in Fig. 12 (a), where the chains are loosely touching with each other. This is a marked difference from the case of Fig. 10(a). The aforementioned monoglobular phase at the low temperatures is directly observed in Fig. 12(b). Small droplets around the globule do not include the chains, but are actually aggregates of salt ions. We infer by Figs. 10 and 12 that the transition from the multiglobular to monoglobular phases occurs at $C_s \leq C_{PA}$, where C_s and C_{PA} are the charge densities of salt ions and polyampholyte, respectively. Once a globule is formed, the monomers inside are arranged discretely like those of neutral polyampholyte in Fig. 4. However, the variance of the filling index in Fig. 11 is large, showing that the tightness of the globules for non-neutral polyampholyte varies considerably, which seems to be characteristic of the salted globules.

Finally, the effect of salt at the fixed temperature $T/T_0 = 0.15$ (the Bjerrum length $\lambda_B \sim 7a$) is shown in Fig. 13. The system gyration radius of non-neutral polyampholyte, with the global charge offset of 40% ($\delta Q/eN^{1/2} = -5.5$), is depicted with solid circles against the number of salt (and counterions). Each data point is an average of four runs of different charge sequences. At $Q_{salt}/Q_{PA} \cong 0.40$, all the free ions are counterions, where Q_{salt} and Q_{PA} are the number of charged particles in salt and polyampholyte, respectively. The open circles in the figure show the system gyration radius for neutral polyampholytes under the same conditions. For the low salt concentrations $Q_{salt}/Q_{PA} < 1$, the system gyration radius stays at the same level as that for the counterion-free neutral polyampholyte. This means that counterion condensation is not significant for the neutral polyampholyte at low salt concentrations. The swelling of neutral polyampholyte at high salt concentration agrees with our previous study [7].

It is interesting that, for non-neutral polyampholyte, the system gyration radius takes a minimum value at $Q_{salt}/Q_{PA} \cong 1$, where about 60% of free ions are absorbed by the polyampholyte, as shown in Fig. 12(a). That is, on top of the counterions, the salt ions condense on the polyampholyte chains at high salt concentration. Then, upon further addition

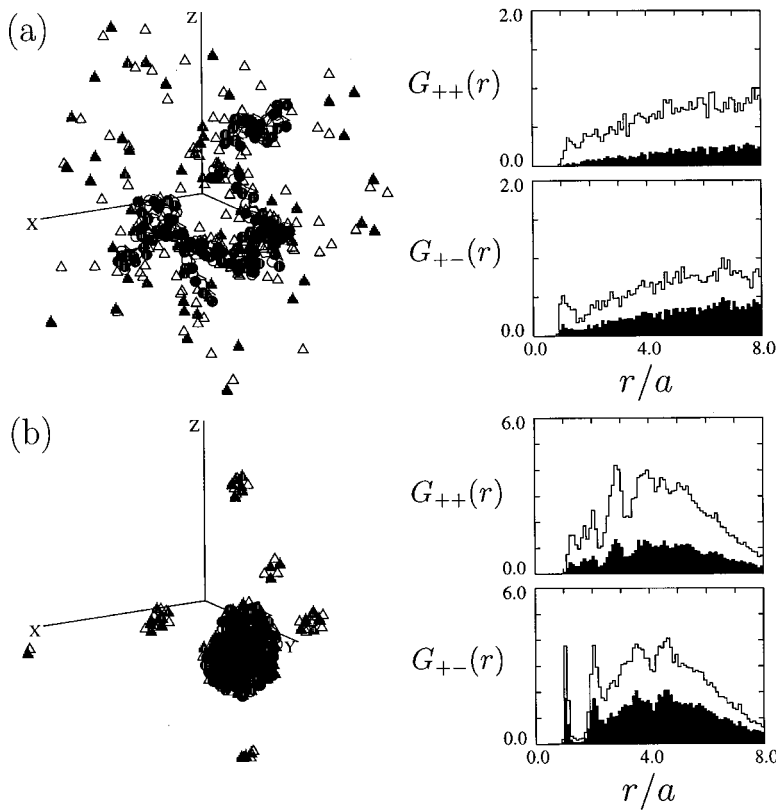


FIG. 12. The bird's-eye view plots (left) and the pair correlation functions (right) are shown for the non-neutral polyampholytes with both counterions and salt (Fig. 11) at the temperatures (a) $T/T_0 \approx 1/5$ and (b) $1/85$. The $G_{++}(r)$ and $G_{+-}(r)$ pair correlation functions are for the pairs of equal-sign and opposite-sign charges, respectively, and the shaded areas are the contribution of the counterions and salt ions.

of salt, the system gyration radius increases, and the whole behavior becomes reentrant. At the salt concentration $Q_{\text{salt}}/Q_{\text{PA}} \sim 1.4$, both neutral and non-neutral polyampholytes approach the non-charged polymer regime.

We believe that the first decrease in the system gyration radius with increasing salt in Fig. 13 is due to better screening of excess charges, in which the polyelectrolyte nature is superseded by that of polyampholyte, whereas the second increase in the system gyration radius is due to a transition from the polyampholyte regime to the noncharged polymer

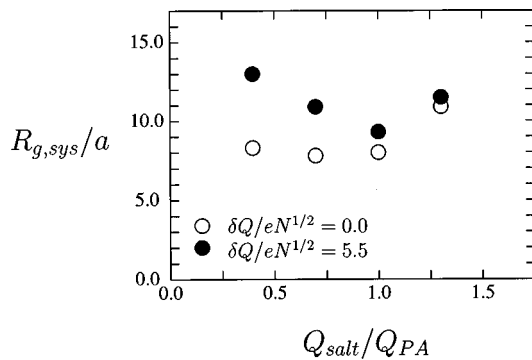


FIG. 13. The effect of counterions and salt at the fixed temperature $T/T_0 = 0.15$ (the Bjerrum length $\lambda_B \sim 7a$) is shown for the six 32-mer polyampholyte with 40% global charge offset $\delta Q/eN^{1/2} \approx -5.5$ (solid circles). The ordinate is the system gyration radius (an average of four runs of different random sequences), and Q_{salt} in abscissa is the total number of free ions (counterions and salt), normalized by that of polyampholyte Q_{PA} . All the free ions are positive counterions at $Q_{\text{salt}}/Q_{\text{PA}} = 0.40$. Shown with open circles is the case for the neutral polyampholyte, where the free ions are half positive and half negative.

regime. We note also that the present molecular dynamics study has reproduced the reentrant behavior of non-neutral polyampholyte against salt ionic strength observed in the experiments of polyampholytic polymers [9] and gels [10,11].

V. SUMMARY

In this paper we studied the condensation and swelling behavior of randomly charged *multichain* polyampholytes in the three-dimensional volume, with the use of molecular dynamics simulations. We specially focused on the structure changes due to the Coulomb coupling parameter (inverse of the temperature) of very wide range, and the effects of counterions and added salt on non-neutral polyampholytes.

Before summarizing our results, we would like to repeat the ways of changing the Coulomb coupling parameter $\Gamma = e^2 Z^2 / \epsilon a k_B T$ (or the Bjerrum length). The change in temperature, the use of polyampholyte with high valence Z , and the solvent of various dielectric constant ϵ , all serve to change the Coulomb coupling parameter. Thus, different regimes of $\Gamma = T_0/T$ ($T_0 = Z^2 e^2 / \epsilon a k_B$) can be studied in a series of experiments while avoiding freezing or vaporization of the solvent. In numerical simulations, a wide range of the Coulomb coupling parameter is accessible for one specific polyampholyte simply by changing temperature. (All the figures were labeled by $T/T_0 = \Gamma^{-1}$.)

In Sec. III we showed that the neutral polyampholyte collapsed to a globule at low temperatures ($\Gamma > 1$), in which the polymer chains penetrated with each other, wiggling through the whole globule. With an increase in temperature, it swelled monotonically to the thermal state where the Coulomb forces played little role. Neutral polyampholyte condensed to an ordered structure of the bcc crystal at very low

temperatures $\Gamma \gg 1$ (Sec. III B). However, the polyampholyte with finitely extensible bonds ended up with a glassy structure that lacked a repeated structure in the long range. Substantial frustrations were retained in the condensed globule, and such polyampholyte was above the global energy minimum due to the bond constraint.

The swelling behavior of non-neutral polyampholytes was examined in Sec. IV. For small global charge offset, i.e., $|\delta Q| < (1/2)eN^{1/2}$, charge complexes (clumps) were formed at low temperatures, which were disintegrated at high temperatures and the polyampholyte became swollen (the polyampholyte regime). This was consistent with theoretical analysis by Everaers, Johner, and Joanny [4] which claimed that polyampholyte is subject to precipitation by the pairing of chains in the distribution tail and oppositely charged majority chains. (The width of the chain distribution $eN^{1/2}$ is comparable to the charge offset δQ .) On the other hand, highly non-neutral polyampholyte was swollen at low temperatures due to Coulombic repulsions, and it shrank to the volume of noncharged polymers at high temperatures (the polyelectrolyte regime).

The effect of counterions and added salt was examined also in Sec. IV. It occurred in two steps: the free ions first weakened the polyelectrolyte nature of non-neutral polyampholyte which caused its collapse. However, the further addition of salt caused transition from the polyampholyte to noncharged polymer regimes, resulting in the swelling of polyampholyte.

Coexisting counterions condensed on unbalanced charge sites of non-neutral polyampholyte (Sec. IV B), but the chains remained separated at all temperatures. Remarkably,

about $N^{1/2}$ counterions did not condense on the polyampholyte but floated in the space around the polyampholyte, down to the temperature $T/T_0 \geq 0.07$. Bare charges of $eN^{1/2}$ remained on the polyampholyte. Therefore, the Debye-Hückel theory was not applicable to the strongly coupled system with $\Gamma \geq 1$ (i.e., low temperatures $T/T_0 < 1$). At low temperatures, the counterions were completely absorbed by globules.

The addition of salt (and counterions) whose charge density was comparable to that of polyampholyte further compactified non-neutral polyampholyte, and a monoglobular phase was reached at very low temperatures (Sec. IV C). The transition from the multiglobular to monoglobular phases occurred at $C_s \lesssim C_{PA}$, where C_s and C_{PA} are the densities of salt ions and polyampholyte, respectively. However, a further increase in salt ionic strength weakened the polyampholyte effect, leading to the swelling of polyampholyte. This reentrant behavior of non-neutral polyampholyte with ionic strength agreed with the experiments for polyampholytic polymers and gels.

ACKNOWLEDGMENTS

One of the authors (M. T.) is highly grateful to Professor A. Yu Grosberg and Professor I. Ohmine for valuable comments and warm encouragements. He also appreciates the fruitful discussions of salt-added polyampholytes with Professor J. F. Joanny, Professor S. J. Candau, and Professor F. Candau in Strasbourg and Professor K. Kremer, Dr. C. Holm, and Dr. R. Everaers in Mainz. Numerical computations for this work were performed on the VPP800 machine at the Institute for Space and Aeronautical Science of Japan.

-
- [1] F. Candau and J.-F. Joanny, *Encyclopedia of Polymeric Materials*, edited by J. C. Salomone (Chemical Rubber, Boca Raton, 1996), Vol. 7, p. 5476.
- [2] P. G. Higgs and J.-F. Joanny, *J. Chem. Phys.* **94**, 1543 (1990).
- [3] A. V. Dobrynin and M. Rubinstein, *J. Phys. II* **5**, 677 (1994).
- [4] R. Everaers, A. Johner, and J.-F. Joanny, *Europhys. Lett.* **37**, 275 (1997).
- [5] Y. Kantor, M. Kardar, and H. Li, *Phys. Rev. E* **49**, 1383 (1994).
- [6] M. Tanaka, A. Yu Grosberg, V. S. Pande, and T. Tanaka, *Phys. Rev. E* **56**, 5798 (1997).
- [7] M. Tanaka, A. Yu Grosberg, and T. Tanaka, *J. Chem. Phys.* **110**, 8176 (1999).
- [8] T. Soddemann, H. Shiessel, and A. Blumen, *Phys. Rev. E* **57**, 2081 (1998).
- [9] J. M. Corpart and F. Candau, *Macromolecules* **26**, 1333 (1993).
- [10] A. E. English, S. Mafe, J. A. Manzanares, X. H. Yu, A. Yu Grosberg, and T. Tanaka, *J. Chem. Phys.* **104**, 8713 (1996).
- [11] G. Nisato, J.-P. Munich, and S. J. Candau, *Langmuir* **15**, 4236 (1999).
- [12] R. C. Gann, S. Chakravarty, and G. V. Chester, *Phys. Rev. B* **20**, 326 (1979).
- [13] H. Thomas, G. E. Morfill, and V. Demmel, *Phys. Rev. Lett.* **73**, 652 (1994).
- [14] H. Totsuji, T. Kishimoto, and C. Totsuji, *Phys. Rev. Lett.* **78**, 3113 (1997).
- [15] D. H. Van Winkle and C. A. Murray, *Phys. Rev. A* **34**, 562 (1986).
- [16] M. O. Robbins, K. Kremer, and G. S. Grest, *J. Chem. Phys.* **88**, 3286 (1986).
- [17] U. Micka, C. Holm, and K. Kremer, *Langmuir* **15**, 4033 (1999).
- [18] M. Stevens and K. Kremer, *J. Phys. II* **6**, 1607 (1996).
- [19] T. Darden, D. York, and L. Pedersen, *J. Chem. Phys.* **98**, 10 089 (1993).
- [20] M. Deserno and C. Holm, *J. Chem. Phys.* **109**, 7678 (1998).
- [21] M. Tanaka, A. Yu Grosberg, and T. Tanaka, *Slow Dynamics in Complex Systems*, edited by M. Tokuyama and I. Oppenheim, AIP Conf. Proc. No. 469 (American Institute of Physics, Woodbury, NY, 1999), p. 599.
- [22] P.-G. de Gennes, *Scaling Concepts in Polymer Physics* (Cornell University Press, Ithaca, 1979).
- [23] J. Ray and G. S. Manning, *Macromolecules* **30**, 5739 (1997).
- [24] E. Y. Kramarenko, A. R. Khokhlov, and K. Yoshikawa, *Macromolecules* **30**, 3383 (1997).